



Published in final edited form as:

Carbohydr Polym. 2020 October 15; 246: 116519. doi:10.1016/j.carbpol.2020.116519.

Hot Melt Extrusion paired Fused Deposition Modeling 3D Printing to Develop Hydroxypropyl Cellulose based Floating Tablets of Cinnarizine

Anh Q. Vo^{a,c}, Jiaxiang Zhang^a, Dinesh Nyavanandi^a, Suresh Bandari^a, Michael A. Repka^{a,b,*}

^aDepartment of Pharmaceutics and Drug Delivery, School of Pharmacy, The University of Mississippi, University, MS 38677, USA.

^bPii Center for Pharmaceutical Technology, The University of Mississippi, University, MS 38677, USA.

^cCurrent Affiliation: Hanoi University of Pharmacy, Department of Physical Chemistry and Physics, Hanoi, Vietnam.

Abstract

Three-dimensional printing could serve as a platform to fabricate individualized medicines and complex-structured solid dosage forms. Herein, hot melt extrusion was coupled with 3D printing to develop a unique gastro retentive dosage form to personalize treatment of cinnarizine or other narrow absorption window drugs. The mechanical strength of the extruded strands was optimized for printing by combining two polymers, hydroxypropyl cellulose and vinylpyrrolidone vinyl acetate copolymer. The unit dose, floating force, and release profile were controlled by the printing parameters and object design. The tablets floated immediately within the FaSSGF, and floating force was relatively constant up to 12 h. Drug release followed zero-order kinetics and could be controlled from 6 h to 12 h. Input variables had a good correlation ($R > 0.95$) with unit dose, floating force, and dissolution profile ($p < 0.05$). Authors successfully proposed and tested a new paradigm of individualized medicine fabrication to meet individual patient needs.

Graphical abstract

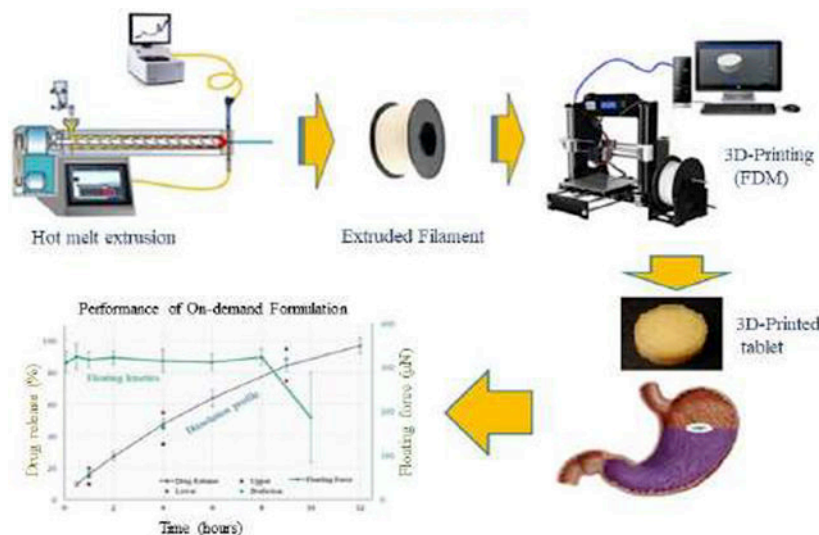
* **Corresponding author:** Michael A. Repka, D.D.S., Ph.D., Distinguished Professor and Chair, Department of Pharmaceutics and Drug Delivery, Director, Pii Center for Pharmaceutical Technology, School of Pharmacy, University of Mississippi, University, MS 38677, USA, Phone: 662-915-1155, Fax: 662-915-1177; marepka@olemiss.edu.

Author Contributions

Anh Q. Vo, Jiaxiang Zhang and Michael Repka designed the study. Anh Q. Vo, Jiaxiang Zhang, performed the experiments and analyzed data. Anh Q. Vo wrote the manuscript, initial review and editing by Dinesh Nyavanandi, Suresh Bandari; final editing by Suresh Bandari, supervision and final approval by M.A. Repka. All authors have given approval to the final version of the manuscript.

Publisher's Disclaimer: This is a PDF file of an unedited manuscript that has been accepted for publication. As a service to our customers we are providing this early version of the manuscript. The manuscript will undergo copyediting, typesetting, and review of the resulting proof before it is published in its final form. Please note that during the production process errors may be discovered which could affect the content, and all legal disclaimers that apply to the journal pertain.

Declaration of interest: none



Keywords

3D printing; Printlet; Individualized medicine; Floating Drug Delivery System; Hot Melt Extrusion

1. Introduction

The development of personalized medicine has been scientifically documented and is becoming a prominent (Garber & Tunis, 2009; Ng, Murray, Levy, & Venter, 2009; Tremblay & Hamet, 2013). “Personalized medicine” can be defined as the tailoring of treatments by 1) identifying patient groups with different responses based on genomic effects, or 2) dosing and delivery of medicines to individuals in a safe and effective manner (Alomari, Mohamed, Basit, & Gaisford, 2015). Bio-variation, which is related to the latter approach, is the most widely recognized cause of treatment variability. The responses of an individual to a drug are dependent on different factors, such as race, age, gender, weight, diet, and inter-subject variation. Some patients are more sensitive to a specific drug or have lesser metabolizing capacity than others. Approximately 80% of adverse effects owing to drug intake are related to inappropriate dose or combination doses (Cohen, 1999). Maximizing the efficacy and safety of drugs administered to every patient is thus a priority of modern health care. Thereby, personalized treatment is among the most efficient strategies. Individualizing treatment for a large population is advantageous and requires a new manufacturing paradigm to replace current pharmaceutical industry approach for mass production. An ideal manufacturing platform for personalized treatment should be safe, highly adjustable, affordable, and controllable by network (Skowyra, Pietrzak, & Alhnan, 2015).

Three dimensional (3D) printing is a novel approach in the fabrication of highly tailorable dosage forms that aim to individualize treatment (Capel, Rimington, Lewis, & Christie, 2018) and frontline care (Trenfield, Awad, Goyanes, Gaisford, & Basit, 2018). Such technique inherently satisfies the requirements of a platform for individualized medicine fabrication. Advantages of 3D printing relative to traditional pharmaceutical manufacturing

include tailoring the dose and composition of each medicinal unit as well as the fabrication of complex structures. Numerous dosage forms have been successfully prepared using printing technology, such as fast disintegration tablets, oral films, controlled release dosages, immediate release tablets, implants, and multiple geometry dosage forms (Kallakunta et al., 2019; Zhang, Vo, Feng, Bandari, & Repka, 2018). The advantage of onsite fabrication capability is predicted to trigger a change from a “one unit dose for all” manufacturing approach to personalized medicine, prepared in pharmacies or hospitals (Alomari et al., 2015).

Among the 3D printing techniques, fused deposition modeling (FDM) 3D printing is the most popular because of its affordability, bench top, highly controllable equipment, (Alhnan et al., 2016; Hsiao, Lorber, Reitsamer, & Khinast, 2018) and more importantly, its use of pharmaceutical polymers to manufacture filaments for printing (Melocchi et al., 2016; Zhang et al., 2019). In FDM 3D printing, a thermoplastic cylindrical filament is pushed by a feeding gear through a heated nozzle, then deposited layer by layer on the printing platform. To use the FDM 3D printing, a formulation should be homogenized and shaped as a uniform filament with suitable mechanical properties. Hot melt extrusion (HME) is the most popular technique in polymer processing and can be utilized to blend drugs with polymers and extrude the formulation through a circular orifice to form a rod shaped filament for FDM 3D printing. Conjugating HME and FDM 3D printing is a viable approach for the fabrication of medicines based on patient needs (Awad, Trenfield, Gaisford, & Basit, 2018).

Many drug candidates are poorly soluble, and their absorption sites are limited to the upper small intestine (Vasconcelos, Sarmiento, & Costa, 2007). Additionally, both the anatomy and internal environment largely differ between gastrointestinal segments that crucially influence the *in vivo* dissolution and absorption of drugs, especially with compounds that have pH-dependent solubility. Ideally, drugs are completely dissolved and absorbed before they are transported through the small intestine (Vo et al., 2017). However, the retention time of the dosage forms in the upper GI tract is relatively short, which might affect the complete absorption of drugs that have an absorption window. Subsequently, drug bioavailability is low and treatment efficacy is poor. Gastroretentive dosage forms, which reside in the stomach and facilitate the transport of drugs through optimum absorption region in dissolved molecules, are a potential solution to these issues. Further, a floating drug delivery system is among the most practical approach to prolong gastric retention time of a dosage form (Singh & Kim, 2000) and is supported by numerous *in vivo* studies (Chai et al., 2017; Ingani, Timmermans, & Moës, 1987; Tadros, 2010; Wen et al., 2019; Whitehead, Fell, Collett, Sharma, & Smith, 1998). Recently, FDM 3D printing has been utilized to fabricate floating aid devices (Charoenying et al. 2020; Fu et al. 2018; Shin et al. 2019), floating pulsatile tablets (Reddy Dumpa et al. 2020) and floating control release matrixes (Chai et al. 2017; Giri et al. 2020). Commercial filaments or HME extruded strands were used as “inks” for FDM 3D printing.

The current study aimed to utilize the advantages of coupling HME and 3D printing to develop floating tablets of cinnarizine utilizing hydroxypropyl cellulose as key polymer. The complex structure tablets, which are difficult to manufacture by traditional pharmaceutical technologies, were designed and printed onsite using “pharmaceutical ink” prepared by

HME. The novelty of this proposed investigation includes the dosage form unique structure and the ability to fabricate personalized medicine based on prescription inputs and patient needs to achieve effective therapy. Fabrication can be optimized by utilizing established regression models. Further, the optimized parameters could control the printing process to manufacture medicines with a desired performance onsite, at a hospital, or pharmacy within several hours.

2. Material and methods

2.1 Materials

Cinnarizine (CIN) was purchased from VWR (Radnor, PA, USA). Hydroxypropyl cellulose (HPC, Klucel MF) was kindly provided by Ashland, Inc. (Lexington, KY, USA).

Vinylpyrrolidone vinyl acetate copolymer (ratio 60:40; Kollidon VA64) was donated by BASF (Ludwigshafen, Germany). HPLC solvents and all other reagents were of analytical grade and purchased from Fisher Scientific (Pittsburgh, PA, USA).

HPC is a cellulosic ether formed by reacting alkali cellulose with propylene oxide. Propylene oxide is substituted on hydroxyls present on each anhydrous monomer unit of cellulose through an ether linkage (Supplement Figure 1). It is available in different grades with varying viscosities and molecular weights ranging from 40,000 to 1,150,000 Daltons. We used HPC MF grade, where M indicates the viscosity type and F indicates that it is of pharmaceutical grade. The Brookfield viscosity (2% in water) for HPC MF grade is 4000–6500 mPa·s with a molecular weight of 850,000 Daltons. HPC is soluble in water at a temperature below 45 °C and readily soluble in many organic solvents. The glass transition temperature of HPC is approximately 120 °C.

Kollidon VA 64 is a random copolymer of vinylpyrrolidone and vinyl acetate. It is manufactured by free radical polymerization of N-vinylpyrrolidone and vinyl acetate with molecular ratio 6:4. Kollidon VA 64 is a pharmaceutical grade polymer, which specifications can be found in major pharmacopoeias (e.g. USP, Ph. Eur., JP). This excipient is available as a spray-dried powder which possesses relatively fine particle size. It is soluble in water, alcohols and other popular hydrophilic solvents. The average molecular weight (M_w) of Kollidon VA 64 is 45000 to 70000 Daltons and its T_g is about 104–109 °C.

2.2 Thermal analysis

Thermogravimetric Analysis (TGA) and Differential Scanning Calorimetry (DSC) were used to confirm the thermal stability of the materials and the drug-loaded filaments during extrusion and FDM, respectively. The pure components, complete physical mixture, and filaments were subjected to TGA experiments using TGA Q 500 (TA Instrument, New Castle, DE, USA). Approximately 8–10 mg of samples were weighed in a platinum pan and heated from 25 °C to 250 °C at ramp rate 10 °C/min. The TGA system was purged with ultrahigh purity nitrogen at a flow rate 40 ml/min to achieve balancing and 60 ml/min for the furnace. The weight lost (percentage of mass remaining) versus temperature change was monitored.

The DSC experiments were performed with a Discovery DSC 2500 system (TA Instrument, New Castle, DE, USA) to confirm the TGA results. Samples weighing 5–10 mg were loaded and sealed in hermetic aluminum pans, and then subjected to equilibrium at 0 °C for 2 min followed by heating from 0 °C to 200 °C at a ramp rate of 10 °C/min in an ultrahigh purity nitrogen environment at a purging flow of 50 ml/min. The heat flow difference between the sample pan and empty pan was monitored and plotted over the temperature change using TA Instruments Trios software. The thermograms were analyzed for unanticipated thermal events.

2.3 Texture analysis

The mechanical strength and brittleness of the extruded filaments were evaluated using a TA-XT2i Texture Analyzer (Stable Micro Systems Ltd., Godalming, England) equipped with a TA-92 adjustable 3 pt bend/snap fixture module (Zhang et al., 2019). The test was carried out with the following parameters: gap between sample support ridges, 12 mm; pre-test speed, 2 mm/s; test speed, 2 mm/s; post-test speed, 10 mm/s; probe moving distance, 10 mm; and resistance force required to trigger the calculation 0.1 N. Briefly, straight extruded strands were collected and cut into 3 cm segments before testing. Each filament segment was placed on the sample holder perpendicular to the blade and the two sample support ridges. The blades moved 10 mm from the trigger point. The resistant force over the distance (or time) was monitored and plotted with the Exponent software version 6.1.5.0 software (Stable Micro Systems Ltd, Godalming, UK). Tensile strength, uniform strain, strain to fracture, fracture stress, and Young's modulus were calculated. The testing for each filament was repeated 5 times.

2.4 Extrusion

Before weighing, aggregates and clumps in each raw material were removed via sieving with a USP #35 mesh screen. Extrusion formulations were prepared and homogeneously mixed. The filaments used for 3D printing were prepared using HME. Briefly, the HME system comprised a twin-screw co-rotating extruder (Process 11™, Thermo Fisher Scientific, Odessa, TX, USA), equipped with 1.5 mm circular die insert, a chiller, a feeder, and a conveyor belt. A Thermo Fischer standard screw configuration at constant screw speed and feed rate of 100 rpm and 8 g/min, respectively, was used for filament extrusion. The temperature of all zones on the barrel and die was set at 130 °C.

Before processing, the extruder was heated to 130 °C and allowed to thermally equilibrate for 15 min. Approximately 30 g of the initial amount of the extrudate was discarded and uniform extrudate strands were collected during steady-state extrusion. To obtain a uniformly-extruded filament with the desired diameter (1.7 ± 0.5 mm), the hot soften extrudate was stretched by adjusting the conveying belt speed to synchronize with the extrudate formation rate. Once the extrudate was processed through the conveying belt, the cool hard extrudate strand was collected in rolls. The extrudate filaments were then stored in air-tight plastic bags in a desiccator to avoid any moisture pickup before 3D printing of the floating tablets was performed.

2.5 FDM 3D printing

The cylindrical hollow tablet models with different wall/vacant space ratios were designed using 3D Builder (Microsoft, Redmond, WA, USA). The models were then sliced and converted to g-code format files using the Cura version 15.04 software (Ultimaker, Geldermalsen, The Netherlands). Tablets were printed with the extruded filaments using a Prusa i3 FDM-3D printer (Prusa Research, Prague, Czech Republic) equipped with an E3D v6 Hot End extruder and a standard 0.4 mm nozzle. The floating tablets were printed with standard resolution, the raft option was activated, and the printing temperature was 165 °C (nozzle temperature). The following printing parameters were employed: print bed temperature, 40 °C; nozzle traveling speed, 70 mm/s; and layer height, 0.10 mm. Printing fill %, shell thickness, and top/bottom thickness were set according to the design of experiments (DoE). The optimized tablets were evaluated for hardness using VK200 Vankel Varian tablet hardness tester (Agilent Technologies, Santa Clara, CA, USA) and friability using friability tester ((Schleuniger Pharmatron, Cleveland, OH, USA).

2.6 Floating strength

The tablet floating force was measured using resultant weight according to the lever principle with the instrumentation and operation described in our previous study (Vo et al., 2016). A five-point calibration curve was established by measuring the resultant weight of the known counterpoise weights. Using a USP dissolution apparatus II (Hanson SR8), floating tablets were placed in 900 mL fasted state simulated gastric fluid (FaSSGF) at 37 ± 0.5 °C and continuously stirred at 50 rpm. At predetermined time points, the resultant weight was measured, and floating strength was calculated by inserting the resultant weight values into the regression equation from the calibration curve.

2.7 Experimental design

The Box-Behnken model was used to derive the experimental plan and correlate the printing structure and tablet dimension with the dissolution kinetics, buoyancy, and unit dose of the floating tablets. The correlation between printing parameters and the performance of the floating tablets could be mathematically described by regression equations, which could be used to determine printing parameters based on the predetermined properties of the tablets. The printed tablets could thus be customized according to individual patient needs. The experimental data were processed using Modde 8.0 software (Umetrics Inc., Sweden). Two DoEs were separately applied to correlate printing structure and tablet dimension to tablet buoyancy, drug release kinetics, and its unit dose. The input parameters were printing structure, such as shell thickness, top/bottom thickness, and print fill %, and tablet dimensions, such as diameter, height, and wall thickness.

2.8 Scanning Electron Microscopy (SEM)

The printing tablets were cut horizontally for SEM examination. The crosscut samples were fixed on aluminum stubs and coated in an inert gas environment comprising ultrahigh purity nitrogen. The samples were coated with gold using a Hummer® 6.2 Sputtering System (Anatech LTD., Battlecreek, MI, USA). The cross-section topography was examined using

SEM at an accelerating voltage of 5 kV and a magnification of 45× (JEOL JSM-5600; JEOL, Inc., Peabody, MA, USA).

2.9 HPLC analysis

CIN was analyzed using a Waters 600 HPLC system (Waters Corp., Milford, MA, USA) equipped with an autosampler, UV/VIS detector, and a Phenomenex® Luna C18 column (5 µm, 250 mm × 4.6 mm). The mobile phase was a mixture of acetonitrile:water (70:30 v/v) adjusted to pH 2 using orthophosphoric acid. Elution was performed in isocratic mode at a flow rate of 1.0 mL/min. The injection volume was set at 20 µL and the signal was detected at a wavelength of 229 nm. Data were collected and processed using the Power software suite.

2.10 *In Vitro* drug release studies

The 3D printed floating tablets were subjected to a dissolution test in 900 mL FaSSGF, a biorelevant dissolution medium whose composition was described by Marques (Marques, Loebenberg, & Almukainzi, 2011) and Jantratid (Jantratid, Janssen, Reppas, & Dressman, 2008). The USP dissolution apparatus type 2 (Hanson SR8; Hanson Research, Chatsworth, CA, USA) was used at a setting temperature of 37 ± 0.5 °C and a paddle rotation speed of 100 rpm. At predetermined time points, 2.0 mL of the sample was withdrawn and 2.0 mL of fresh dissolution medium was added. Subsequently, the samples were filtered through 0.2 µm, 13 mm PTFE membrane (Whatman, Inc., Haverhill, MA, USA), and diluted with an equal volume of acetonitrile. Thereafter, a 20-µL volume of the diluted solution was injected into the HPLC system for analysis.

3 Results and Discussion

3.1 Thermal analysis

CIN was used as a model drug while HPC and PVP VA 64 were used as the matrix-forming polymers. Two thermal processes, namely HME and fused deposition 3D printing, were involved in the fabrication of floating tablets. Therefore, thermal stability was critical for establishing the processing conditions, and processing temperature had to be lower than the degradation temperature.

Thermal analysis was utilized to evaluate the thermal stability of the formulation during extrusion and printing. Initially dry nitrogen flow transported the sample moisture, causing weight lost before 100 °C in the TGA thermograms (Supplement Figure 2a). The API and PVP VA 64 began to degrade at a detectable rate at approximately 190–200 °C and degraded above 200 °C; however, HPC was stable at least up to 250 °C. The physical mixture of the formulation was stable up to 200 °C. Extrusion was performed at 130 °C, which is far below the degradation temperature of the formulation, to ensure the formulation was stable after the filament extrusion. The extruded filament was stable up to 200 °C, which was well above the printing temperature of 165 °C. These observations confirmed the suitability of the processing temperature. The DSC results (Supplement Figure 2b) provided more evidence to confirm the thermal stability of the materials and filaments to support the TGA experimental results. There was no detectable thermal event, except the melting peak of CIN at

approximately 123 °C on the thermogram of the pure drug. To maximize the stability of the formulations during the thermal processes, the operation temperatures of extrusion and printing were optimized by selecting the lowest temperature, 130 °C for extrusion and 165 °C for printing, to allow smooth performance of the process in a steady state. Below 160 °C, the printing nozzle was clogged with the materials. Thus, the thermal analysis results indicated that the processing temperatures were well below the starting point of thermal degradation, and thus, formulations would be stable during the processes.

Compared to the theoretical values, drug content of the filaments and the printed tablets was 97.55 – 101.02% and 97.81–99.85%, respectively. No impurity or strange peak was identified on any of the chromatograms.

3.2 Filament preparation

Two approaches were previously reported for the preparation of drug-loaded filaments for FDM 3D printing, namely drug impregnation and melt extrusion. The former method is related to the loading of a drug into a commercial filament via soaking in a drug solution for a sufficient length of time. After solvent removal, a uniform printable filament is obtained (Goyanes, Buanz, Basit, & Gaisford, 2014). However, this process is time consuming, drug loading of the filament is low, and its application is limited. In the latter approach, a physical mixture of drugs and matrix forming polymers is extruded to form a cylindrical strand, which can be used as a filament for FDM 3D printing. Such method could create relatively high drug-loaded filaments and is compatible with a wide range of materials. Different pharmaceutical grade polymers have been successfully utilized to fabricate filaments for 3D printing (Melocchi et al., 2016; Zhang et al., 2019). Two important physical properties of a filament are stiffness and ductility, and they are often employed to determine whether an extruded strand can be used as a filament in an FDM 3D printer. HPC was used as the main matrix-forming polymer owing to its low T_g, implying that the formulations could be processed at a relatively low temperature (Melocchi et al., 2016). However, the extruded strand of the CIN and HPC mixture was soft. Thereby, the filament was squeezed under the push of the feeding gear of the 3D printer. After multiple screening experiments, PVP VA 64 was selected as the co-matrix forming polymer. The combination of HPC and PVP VA 64 significantly improved the texture properties of the extruded filament and made it printable. The formulations were extruded using a hot melt extruder to obtain 1.7-mm uniform strands which were later used as filaments for 3D printing. Extrusion shaped the formulations as circular strands by pumping the molten mass through a circular orifice attached to the die of the extruder. Extrusion was performed at 130 °C, which was the lowest temperature that allowed the establishment of a steady process of extrusion. A standard screw configuration with 3 mixing zones was used while feed rate and screw speed were selected in the range of a typical extrusion process at a lab scale. Extrusion ran smoothly and steadily with relatively low torque (10–15%) and die pressure (17–21 bar). The conveying belt speed was adjusted to stretch the molten extrudate swelling at the die orifice to obtain a 1.7-mm uniform strand. Because the processing temperature was higher than the drug melting point (130 °C compared to 122 °C), the API was melted during extrusion and served as a process aid (plasticizer/lubricant) that helped to reduce the torque. The extrusion ran as a missibilization regime which facilitated the dispersion of the melted API in the polymer matrix and

transformation of API to the amorphous form (Repka et al., 2018). All extruded filaments were translucent and could be collected as “roll of ink” (Figure 1) for use to continuously print multiple tablets.

A 3-point bend (Repka – Zhang) test was used to evaluate the physical properties of the filaments. The tensile strength, uniform strain, and modulus of rigidity revealed filament strength while the fracture stress and strain to fracture revealed its ductility. Filaments were required to possess a suitable strength and good ductility as they would experience a certain degree of deformation during printing. The effects of PVP VA 64 on the physical strength of the filament are presented in Table 1. Increasing the PVP VA 64 ratio resulted in a stronger but more brittle filament as shown in Figure 1E. Additionally, the filaments with a strain to fracture greater than 150% would not break during printing, and a tensile strength greater than 2.5 N/mm² would prevent distortion (squeezing) of the filament by the feeding gear. The filaments with a PVP VA 64 content >30% were frequently broken at the feeding gear and squeezed if the PVP VA 64 content was <10%. Incorporating 15–25% of PVP VA 64 into the formulation improved the extrudate physical properties, resulting in printable filaments. From the above results, the formulation with 20% PVP VA 64 content was selected to prepare the filament for later experiments. The extruded filament was uniform cylindrical with a diameter of approximately 1.7 mm and possessed a dense internal structure and a smooth surface (Figure 1), indicating its ease for feeding into the printing nozzle. The strand could be collected as ink rolls, enabling mounting on the 3D printer to continuously fabricate multiple objects.

3.3 Tablet design and printing

Before printing, the object was designed, sliced into a multiple layer model, and transformed into the .gcode format using suitable softwares. “Ink”, which is used in FDM 3D printing, is a thermoplastic polymer filament that is pushed through a heated nozzle by a two-roller gear. The tip of the filament is in situ melted at the nozzle. The filament pushed by feeding gears acts as a piston to pump out the molten mass which is deposited layer by layer on the printing platform. Printing is controlled by parameters such as nozzle temperature, nozzle moving speed, layer heights, shell thickness, top/bottom thickness, and infill density.

The advantages of 3D printing relative to traditional pharmaceutical manufacturing technologies were leveraged to fabricate tablets with complex structure. The floating tablets were designed as hollow cylindrical objects as shown in Figure 2. Such low-density dosage forms enable floating over the gastric fluid. Additionally, a low infill density of the tablet wall could also contribute to the buoyancy of the tablet. The drug release profile of the tablets was defined by the shell thickness, wall thickness, wall structure, and the object design, which controlled the weight, and hence, the dose of the floating tablets. Briefly, the buoyancy, dose, and drug release kinetics of the dosage form could be tailored by a few mouse clicks based on the established correlation between those input parameters and tablet performance.

Two sets of experimental design were employed to determine the correlations between independent variables and the tablet performance, including buoyancy, unit dose, and release kinetics. The first DoE focused on the effects of the tablet structure, which were controlled

by printing parameters, while the second DoE sought to investigate the influences of device dimension, which was customized by model design. From preliminary studies, independent variables and their variation ranges were determined as shown in Supplement Table 1. Thirty DoE formulations were successfully fabricated following precisely designed models through a smooth printing process. Once in contact with the dissolution media, a gel layer was formed at the tablet surface that could control dissolution media penetration into the matrix and drug release, and maintain the vacancy inside the matrix. All prepared tablets floated immediately within the FaSSGF and the buoyancy was maintained from 6 h to more than 12 h. More than 80% of the drug was released.

3.4 Effect of internal structure on buoyancy and dissolution profile of the floating tablets

A Box-Behnken DoE consisting of 15 formulations (Table 2) was executed to evaluate the impact of the tablet internal structure (controlled by printing parameters) on the performance of dosage form. The tablet model was hollow and had a diameter of 10.0 mm, height of 6.5 mm, and wall thickness of 2.5 mm. The printing parameters, namely infill, top/bottom thickness, and shell thickness defined the internal structure of the tablet and thus controlled the drug release profile and floating kinetics. The infill parameter defined the percentage of the printing space that would be filled with “ink”. This variable could be set from 0%, corresponding to the no printing material deposited, to 100%, where the printing materials completely fill the printing space. Shell and top/bottom defined the thickness of the outer layer which filled with the highest density of printing material, higher than 100% fill (Zhang et al., 2017). They were discrete variables that were varied by steps of 0.1 mm (printing resolution) and 0.4 mm (nozzle diameter) for the top/bottom and shell variables, respectively.

The printing parameters influenced the density and penetration of the dissolution media into the tablets, thereby controlling the drug release profile and floating kinetics. Shell and top/bottom layers created a tight structure, retarding the dissolution media penetrated into the tablets. Therefore, this layer swelled relatively slower and formed a relatively dense gel layer that impeded drug release. The thicker the shell and top/bottom, the slower the drug release and the longer the maintenance of buoyancy. However, the inner structure was loose, thereby enabling a more rapid swelling of the polymer. Additionally, the existence of numerous channels, where infill was <100%, facilitated the penetration of the dissolution media toward the tablet core to further accelerate drug release from the matrix. The performance of the DOE formulations, including floating force and dissolution at 1 h, 4 h, and 9 h, is presented in Table 2.

All printed tablets floated immediately within the FaSSGF medium and their buoyancy was relatively constant from 6 h to more than 12 h, depending on the formulations (Figure 3a). Thereafter, the tablets quickly lost their buoyancy strength as either the hollow structure was disrupted, or the dissolution medium quickly penetrated the vacant space in the center of the tablets. The floating force of the tablets largely varied between the formulations (Figure 3a).

The regression results demonstrated a good correlation between printing parameters and the floating force ($R^2 = 0.990$). Further, the model was dependable for predicting the floating force from the printing parameters ($Q^2 = 0.710$). The correlation was mathematically

expressed by regression equations (coefficients listed in Table 3) and visually depicted by contour plots (Figure 4). All three printing parameters significantly influenced the tablet buoyancy performance ($p < 0.05$) and were contravariant to the floating force. The regression indicated that the shell thickness had the greatest effect and top/bottom thickness had the smallest effect on tablet buoyancy. There were potential interactions between infill and top/bottom thickness ($p < 0.05$) as well as shell and top/bottom thickness ($p < 0.1$).

These printing parameters greatly influenced the drug release kinetics. As shown in the dissolution plots (see Supplement Figure 3), few formulations released 80% in 6 h while other formulations took more than 12 h to achieve 80% release, with less than 50% of the drug being released in 6 h. The printing parameters defined density and pattern of the formulations deposited on the tablet model, thereby controlling the density and thickness of the swelling gel layer which governed the drug release profiles. Shell thickness highly influenced drug dissolution. When the shell thickness was constant at 0.4 mm, the difference in the dissolution profiles among N9-N12 was minimal compared to that among N1-N4 and N5-N8 (Supplement Figure 3). However, when the top/bottom was kept constant at 0.6 mm, the largest variation of the dissolution profiles was observed (N5-N8), implying the least impact of this factor on the drug release profile. Impacts of these parameters could be quantitatively compared via their coefficients of encoded regression equations listed in Table 3. All coefficients of the three parameters were negative; thus, they were contravariant with drug dissolution. The coefficients of the shell thickness were 5-fold (1 h) and 3-fold (4 h and 9 h) greater than those of top/bottom thickness. The effects of the printing parameters could also be visualized by response contours. Subsequently, their effects could be quickly determined from the plots (Figure 4).

The DoE regression results revealed a good correlation between printing parameters and the dissolution of the dosage form ($R^2 > 0.98$). The shell thickness and infill parameters significantly influenced drug release at 1 h, 4 h, and 9 h ($p < 0.05$) while the top/bottom thickness gained significance with time and became significant at the 4 h time point ($p = 0.084$ at 1 h, and $p = 0.014$ and 0.01 after 4 h and 9 h, respectively). The prediction of the regression model was acceptable ($Q^2 > 0.49$), thereby enabling the optimization of these variables for printing tablets with the desired dissolution profiles.

3.5 Effect of design on the performance of floating tablets

The tablet model, which could be tailored by several mouse clicks, was defined by the design parameters including diameter, height, and wall thickness. Beside controlling unit dose, these parameters influenced the surface area and diffusion pathlength, thereby governing the drug release profiles. These parameters also influenced the floating force by defining the vacant space in the tablet core. This set of DoE (Table 4) revealed the correlation between the model design and the unit dose, buoyancy, and dissolution kinetics of the floating tablets while the printing parameters were kept constant (wall thickness = 0.4 mm, infill = 65%, and top/bottom thickness = 0.4 mm). The unit dose, floating force, and dissolution at 1 h, 4 h, and 9 h of the DoE formulations are listed in Table 4.

The DOE results (Table 4) confirmed that tablet diameter, height, and wall thickness significantly influenced the weight of the printed tablets ($p < 0.05$). There was no significant

interaction among these three parameters ($p > 0.05$) meaning they independently controlled the tablet weight. The tablet diameter had the greatest influence on the tablet weight; its coefficient was 2.5-fold higher than the tablet height and 5-fold higher than the wall thickness.

These parameters significantly influenced ($p < 0.05$) the floating force of the dosage form, which was maintained relatively constant until the matrices were disrupted (Figure 3b). Tablet diameter and height had a covariant effect (positive coefficients) on the floating force, while wall thickness had a (negative coefficient) contravariant effect. The tablet diameter had the greatest effect on the floating force displayed by its greatest coefficient in the encoded regression equation.

Additionally, the square of the diameter variable (D^2) significantly influenced the floating force ($p < 0.05$). Potential interactions between diameter and tablet height, and diameter and wall thickness ($p < 0.05$) could also occur, which indicated that the effect of wall thickness and tablet height was dependent on the values of the diameter, and vice versa.

The dissolution kinetics of the printed tablets was contravariant to the three design parameters that could be identified visually using contour plots (Supplement Figure 4) or quantitatively based on the coefficients of the regression equations listed in Table 5. Among the three parameters, tablet height had the least impact on dissolution profile (Supplement Figure 5). When the height was kept constant (formulation D5-D8), the dissolution profile had the largest fluctuation. However, diameter had the greatest impact on dissolution, thereby exhibiting the greatest coefficient. The least variation in dissolution profile was observed when the diameter was kept unchanged in formulations D9-D12.

The regression results indicated an excellent correlation between input factors (diameter, height, and wall thickness of the tablets) and output variables, including tablet weight, floating force, and drug dissolution at 1, 4, and 9 h ($R^2 > 0.95$, $Q^2 > 0.57$). The models were thus deemed dependable ($p < 0.05$) for calculating unit dose, floating force, and dissolution profile from a given set of input variables when the regression equation coefficients listed in Table 5 are used. Conversely, the input variables could be determined to print floating tablets with desired weight, buoyancy, and dissolution profile via optimization with predetermined constraints.

Application of the regression model—Personalized medicines require the tailoring of formulation attributes such as unit dose and drug release kinetics based on individual patient needs. Therefore, establishing a correlation between the fabrication parameters and the performance of a dosage form is a primary requirement that enables the immediate calculation of input variables when a prescription order is received. Otherwise, days or even weeks of experiments would be required to determine the conditions required to fabricate a specific personalized medicine request.

The developed model has been applied to fabricate floating tablets with predetermined attributes and corresponding variation ranges (Supplement Table 2). The elaborated regression was utilized to calculate the input variables of the tablet model using the

optimization function of the software. The object model with predicted outputs closest to the target values revealed a diameter of 10.9 mm, height of 6.2 mm, and wall thickness of 1.7 mm.

The characterization results of the optimized formulation are presented in (Supplement Table 2). The hardness of optimized tablet was observed to be 16.32 ± 1.91 kp and the tablet did not break into pieces. Similarly, the % friability value was well below 0.1 %. The dissolution profile and floating kinetics are plotted in Figure 5. All outputs were within the predetermined variation limits. The experiment value of the output variables was diverse but did not exceed 10% compared to target values and was less than 7% compared to the predicted values. However, the floating force served as an exception, as it had a 13% difference from the predicted value. The dissolution profile of the printed tablets was well within the defined constrains. The tablet weight was lighter than the predicted value, which might be due to the thinner filament utilized. Similarly, the floating force was higher than the predicted value.

Drug release kinetics of the floating tablets—When the floating tablet interacts with the dissolution media, the polymer matrix swells and forms a gel structure that covers the tablet. Herein, drug release was achieved via two mechanisms, diffusion through the gel structure and erosion of the matrix. The drug release kinetics of such controlled release dosage forms has been extensively studied and modeled by Siepmann et al (Siepmann, Kranz, Bodmeier, & Peppas, 1999; Siepmann, Podual, Sriwongjanya, Peppas, & Bodmeier, 1999) and Caccavo et al (Caccavo, Cascone, Lamberti, & Barba, 2015). These models were derived for conventional swelling matrixes that contained swellable materials that were continuously distributed throughout the matrix. According to these models, drug release occurred at a faster rate at the early phase and became slower over time due to the longer diffusion pathlength of the drug in the matrix core and the decrease in the matrix surface. However, as the floating tablets possessed a hollow structure, the drug release kinetics resembled that of the early stage of conventional swellable matrixes due to the absence of a later phase. The empirical equations therefore revealed that the drug release kinetics of different dosage forms (Costa & Sousa Lobo, 2001) could not be applied to these floating tablets.

After an initial minor burst, drug release from the 3D printed tablets followed zero order kinetics ($R^2 > 0.98$, dissolution data from 30 min to a time point where approximately 80% of the drug was released). The relatively constant drug release profile (Supplement Figure 3, 5) derived using the special structure of the floating tablets, which was used to establish the surface and diffusion pathlength of the swelling matrix, was relatively consistent throughout dissolution.

4 Conclusion

A unique floating dosage form was successfully fabricated by coupling melt extrusion with 3D printing. HME showed advantages, such as the generation of high drug-loaded filaments, customization of filament properties, and formulation of pharmaceutical polymer-based filaments, for the manufacture of filaments for FDM 3D printing. The tablet properties,

including its unit dose, floating force, and dissolution profile, could be tailored by several mouse-clicks via customizing the object design or printing the structure of the tablet model. Drug release from the floating tablets followed pseudo zero order kinetics and could be controlled from 6 h to more than 12 h. The tablets could immediately float within the FaSSGF, and the floating force remained constant until 80% of the drug was released. The printing parameters (infill, shell, top/bottom thickness) and object design (diameter, height, wall thickness) had a very good correlation with tablet performance and the regression models were essential for tailoring the dosage forms, thereby satisfying individualized treatment. The proposed floating drug delivery system is a viable approach for establishing individualized treatment of drugs with narrow absorption windows.

Supplementary Material

Refer to Web version on PubMed Central for supplementary material.

Acknowledgments

The authors would like to thank Ashland Inc. for its generous support toward the performance of this project.

Funding

This project was partially supported by the National Institute of General Medical Sciences (NIGMS), a component of the National Institutes of Health (NIH), as one of its Centers of Biomedical Research Excellence (COBRE) [grant number P30GM122733-01A1].

References

- Alhnan MA, Okwuosa TC, Sadia M, Wan KW, Ahmed W, & Arafat B (2016, 8 1). Emergence of 3D Printed Dosage Forms: Opportunities and Challenges. *Pharmaceutical Research*, Vol. 33, pp. 1817–1832. 10.1007/s11095-016-1933-1 [PubMed: 27194002]
- Alomari M, Mohamed FH, Basit AW, & Gaisford S (2015). Personalised dosing: Printing a dose of one's own medicine. *International Journal of Pharmaceutics*, 494(2), 568–577. 10.1016/j.ijpharm.2014.12.006 [PubMed: 25498157]
- Awad A, Trenfield SJ, Gaisford S, & Basit AW (2018, 9 5). 3D printed medicines: A new branch of digital healthcare. *International Journal of Pharmaceutics*, Vol. 548, pp. 586–596. 10.1016/j.ijpharm.2018.07.024 [PubMed: 30033380]
- Caccavo D, Cascone S, Lamberti G, & Barba AA (2015). Modeling the drug release from hydrogel-based matrices. *Molecular Pharmaceutics*, 12(2), 474–483. 10.1021/mp500563n [PubMed: 25495793]
- Capel AJ, Rimington RP, Lewis MP, & Christie SDR (2018, 12 1). 3D printing for chemical, pharmaceutical and biological applications. *Nature Reviews Chemistry*, Vol. 2, pp. 422–436. 10.1038/s41570-018-0058-y
- Chai X, Chai H, Wang X, Yang J, Li J, Zhao Y, Xiang X (2017). Fused deposition modeling (FDM) 3D printed tablets for intragastric floating delivery of domperidone. *Scientific Reports*, 7(1), 1–9. 10.1038/s41598-017-03097-x [PubMed: 28127051]
- Charoenying T, Patrojanasophon P, Ngawhirunpat T, Rojanarata T, Akkaramongkolporn P, Opanasopit P (2020) Fabrication of floating capsule-in-3D-printed devices as gastroretentive delivery systems of amoxicillin. *Journal of Drug Delivery Science and Technology* 55:101393
- Cohen JS (1999, 9). Ways to minimize adverse drug reactions: Individualized doses and common sense are key. *Postgraduate Medicine*, Vol. 106, pp. 163–172. 10.3810/pgm.1999.09.688 [PubMed: 10494273]

- Costa P, & Sousa Lobo JM (2001, 5 1). Modeling and comparison of dissolution profiles. *European Journal of Pharmaceutical Sciences*, Vol. 13, pp. 123–133. 10.1016/S0928-0987(01)00095-1 [PubMed: 11297896]
- Fu J, et al. (2018) Combination of 3D printing technologies and compressed tablets for preparation of riboflavin floating tablet-in-device (TiD) systems. *International journal of pharmaceutics* 549(1–2):370–379 [PubMed: 30107218]
- Garber AM, & Tunis SR (2009). Does comparative-effectiveness research threaten personalized medicine? *New England Journal of Medicine*, 360(19), 1925–1927. 10.1056/NEJMp0901355 [PubMed: 19420360]
- Giri BR, Song ES, Kwon J, Lee J-H, Park J-B, Kim DW (2020) Fabrication of Intragastric Floating, Controlled Release 3D Printed Theophylline Tablets Using Hot-Melt Extrusion and Fused Deposition Modeling. *Pharmaceutics* 12(1):77
- Goyanes A, Buanz ABM, Basit AW, & Gaisford S (2014). Fused-filament 3D printing (3DP) for fabrication of tablets. *International Journal of Pharmaceutics*, 476(1), 88–92. 10.1016/j.ijpharm.2014.09.044 [PubMed: 25275937]
- Hsiao W-K, Lorber B, Reitsamer H, & Khinast J (2018). 3D printing of oral drugs: a new reality or hype? *Expert Opinion on Drug Delivery*, 15(1), 1–4. 10.1080/17425247.2017.1371698 [PubMed: 28836459]
- Ingani HM, Timmermans J, & Moës AJ (1987). Conception and in vivo investigation of peroral sustained release floating dosage forms with enhanced gastrointestinal transit. *International Journal of Pharmaceutics*, 35(1–2), 157–164. 10.1016/0378-5173(87)90084-6
- Jantravid E, Janssen N, Reppas C, & Dressman JB (2008). Dissolution media simulating conditions in the proximal human gastrointestinal tract: An update. *Pharmaceutical Research*, 25(7), 1663–1676. 10.1007/s11095-008-9569-4 [PubMed: 18404251]
- Kallakunta VR, Sarabu S, Bandari S, Tiwari R, Patil H, & Repka MA (2019). An update on the contribution of hot-melt extrusion technology to novel drug delivery in the twenty-first century: part I. *Expert Opinion on Drug Delivery*, 16(5), 539–550. 10.1080/17425247.2019.1609448 [PubMed: 31007090]
- Marques MRC, Loebenberg R, & Almukainzi M (2011). Simulated biological fluids with possible application in dissolution testing. *Dissolution Technologies*, Vol. 18, pp. 15–28. 10.14227/DT180311P15
- Melocchi A, Parietti F, Maroni A, Foppoli A, Gazzaniga A, & Zema L (2016). Hot-melt extruded filaments based on pharmaceutical grade polymers for 3D printing by fused deposition modeling. *International Journal of Pharmaceutics*, 509(1–2), 255–263. 10.1016/j.ijpharm.2016.05.036 [PubMed: 27215535]
- Ng PC, Murray SS, Levy S, & Venter JC (2009, 10 8). An agenda for personalized medicine. *Nature*, Vol. 461, pp. 724–726. 10.1038/461724a [PubMed: 19812653]
- Reddy Dumpa N, Bandari S, A Repka M (2020) Novel Gastroretentive Floating Pulsatile Drug Delivery System Produced via Hot-Melt Extrusion and Fused Deposition Modeling 3D Printing. *Pharmaceutics* 12(1):52
- Repka MA, Bandari S, Kallakunta VR, Vo AQ, McFall H, Pimparade MB, & Bhagurkar AM (2018). Melt extrusion with poorly soluble drugs – An integrated review. *International Journal of Pharmaceutics*, 535(1–2), 68–85. 10.1016/j.ijpharm.2017.10.056 [PubMed: 29102700]
- Shin S, et al. (2019) Development of a gastroretentive delivery system for acyclovir by 3D printing technology and its in vivo pharmacokinetic evaluation in Beagle dogs. *PloS one* 14(5)
- Siepmann J, Kranz H, Bodmeier R, & Peppas NA (1999). HPMC-matrices for controlled drug delivery: A new model combining diffusion, swelling, and dissolution mechanisms and predicting the release kinetics. *Pharmaceutical Research*, 16(11), 1748–1756. 10.1023/A:1018914301328 [PubMed: 10571282]
- Siepmann J, Podual K, Sriwongjanya M, Peppas NA, & Bodmeier R (1999). A new model describing the swelling and drug release kinetics from hydroxypropyl methylcellulose tablets. *Journal of Pharmaceutical Sciences*, 88(1), 65–72. 10.1021/js9802291 [PubMed: 9874704]

- Singh BN, & Kim KH (2000, 2 3). Floating drug delivery systems: An approach to oral controlled drug delivery via gastric retention. *Journal of Controlled Release*, Vol. 63, pp. 235–259. 10.1016/S0168-3659(99)00204-7 [PubMed: 10601721]
- Skowrya J, Pietrzak K, & Alhnan MA (2015). Fabrication of extended-release patient-tailored prednisolone tablets via fused deposition modelling (FDM) 3D printing. *European Journal of Pharmaceutical Sciences*, 68, 11–17. 10.1016/j.ejps.2014.11.009 [PubMed: 25460545]
- Tadros MI (2010). Controlled-release effervescent floating matrix tablets of ciprofloxacin hydrochloride: Development, optimization and in vitro-in vivo evaluation in healthy human volunteers. *European Journal of Pharmaceutics and Biopharmaceutics*, 74(2), 332–339. 10.1016/j.ejpb.2009.11.010 [PubMed: 19932750]
- Tremblay J, & Hamet P (2013). Role of genomics on the path to personalized medicine. *Metabolism: Clinical and Experimental*, 62(SUPPL.1), S2–S5. 10.1016/j.metabol.2012.08.023 [PubMed: 23021037]
- Trenfield SJ, Awad A, Goyanes A, Gaisford S, & Basit AW (2018, 5 1). 3D Printing Pharmaceuticals: Drug Development to Frontline Care. *Trends in Pharmacological Sciences*, Vol. 39, pp. 440–451. 10.1016/j.tips.2018.02.006 [PubMed: 29534837]
- Vasconcelos T, Sarmiento B, & Costa P (2007, 12). Solid dispersions as strategy to improve oral bioavailability of poor water soluble drugs. *Drug Discovery Today*, Vol. 12, pp. 1068–1075. 10.1016/j.drudis.2007.09.005 [PubMed: 18061887]
- Vo AQ, Feng X, Morott JT, Pimparade MB, Tiwari RV, Zhang F, & Repka MA (2016). A novel floating controlled release drug delivery system prepared by hot-melt extrusion. *European Journal of Pharmaceutics and Biopharmaceutics*, 98, 108–121. 10.1016/j.ejpb.2015.11.015 [PubMed: 26643801]
- Vo AQ, Feng X, Pimparade M, Ye X, Kim DW, Martin ST, & Repka MA (2017). Dual-mechanism gastroretentive drug delivery system loaded with an amorphous solid dispersion prepared by hot-melt extrusion. *European Journal of Pharmaceutical Sciences*, 102, 71–84. 10.1016/j.ejps.2017.02.040 [PubMed: 28257881]
- Wen H, He B, Wang H, Chen F, Li P, Cui M, ... Yang X (2019). Structure-Based GastroRetentive and Controlled-Release Drug Delivery with Novel 3D Printing. *AAPS PharmSciTech*, 20(2), 68 10.1208/s12249-018-1237-3 [PubMed: 30627938]
- Whitehead L, Fell JT, Collett JH, Sharma HL, & Smith A (1998). Floating dosage forms: an in vivo study demonstrating prolonged gastric retention. *Journal of Controlled Release : Official Journal of the Controlled Release Society*, 55(1), 3–12. 10.1016/s0168-3659(97)00266-6 [PubMed: 9795000]
- Zhang J, Vo AQ, Feng X, Bandari S, & Repka MA (2018, 11 1). Pharmaceutical Additive Manufacturing: a Novel Tool for Complex and Personalized Drug Delivery Systems. *AAPS PharmSciTech*, Vol. 19, pp. 3388–3402. 10.1208/s12249-018-1097-x [PubMed: 29943281]
- Zhang J, Xu P, Vo AQ, Bandari S, Yang F, Durig T, & Repka MA (2019). Development and evaluation of pharmaceutical 3D printability for hot melt extruded cellulose-based filaments. *Journal of Drug Delivery Science and Technology*, 52, 292–302. 10.1016/j.jddst.2019.04.043
- Zhang J, Yang W, Vo AQ, Feng X, Ye X, Kim DW, & Repka MA (2017). Hydroxypropyl methylcellulose-based controlled release dosage by melt extrusion and 3D printing: Structure and drug release correlation. *Carbohydrate Polymers*, 177, 49–57. 10.1016/j.carbpol.2017.08.058. [PubMed: 28962795]

Highlights:

- Gastroretentive floating tablets were developed using HME coupled FDM 3D printing.
- HPC and PVP VA 64 in combination produced 3D printable filaments.
- Extruded filaments possessed good mechanical strength suitable for 3D printing.
- 3D design of tablets has significant impact on drug release characteristics.
- Buoyancy kinetics of 3D printed floating tablets.

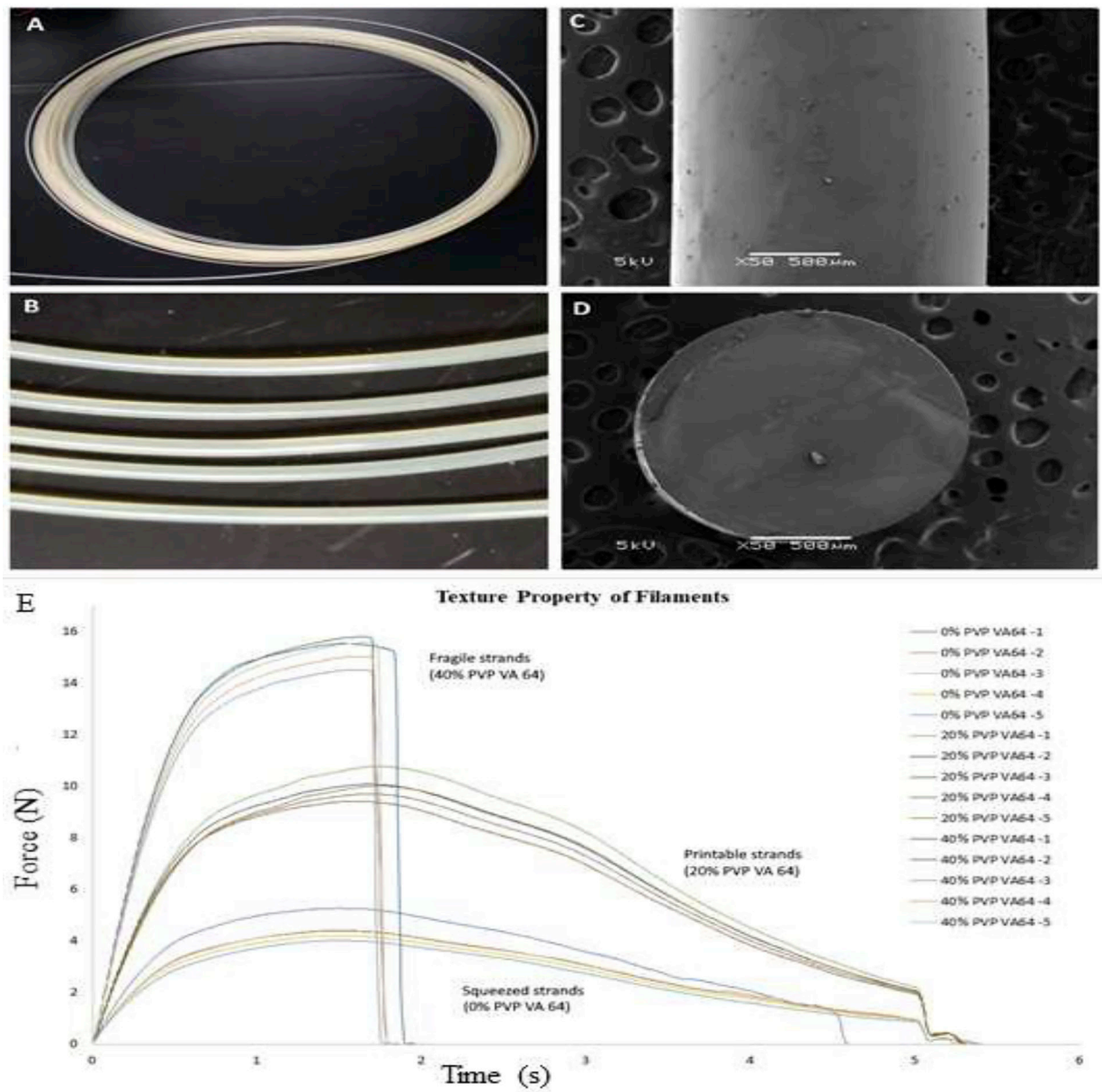


Figure 1: Morphology of the filament A) and B) digital image of the extruded filament collected as an “ink roll”; C) SEM image of the filament surface; D) SEM image of the cross section of the filament; and E) Texture properties of extruded strands tested by using 3 points bend test ($n=5$)

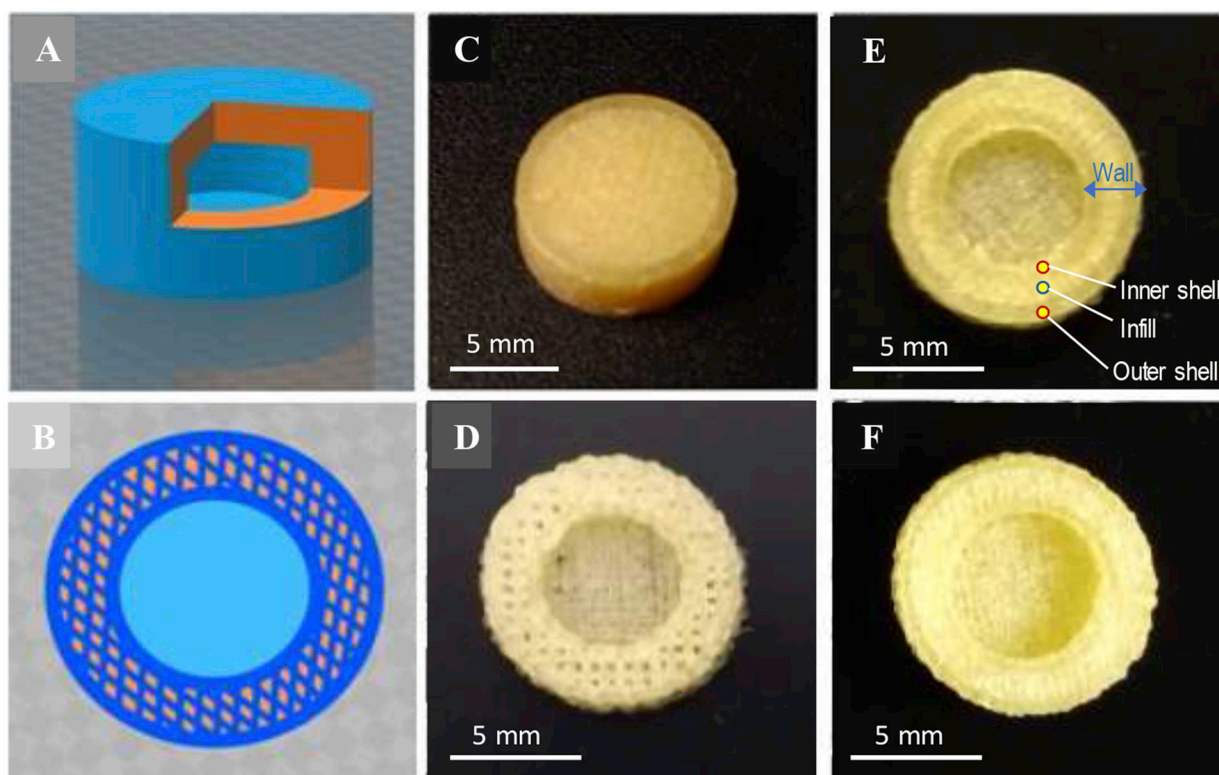


Figure 2:

Image of model tablet and printed tablets. A) The hollow tablet model; B) Design of tablet wall structure; C) representative 3D printed tablet (diameter 10.0 mm, height 6.5 mm, wall thickness 2.5 mm); D) horizontal cross section of the tablet with 50% infill, 0.4 mm shell; E) cross section of the tablet with 80% infill, 0.8 mm shell; F) cross section of the tablet with 80% infill, 0.4 mm shell.

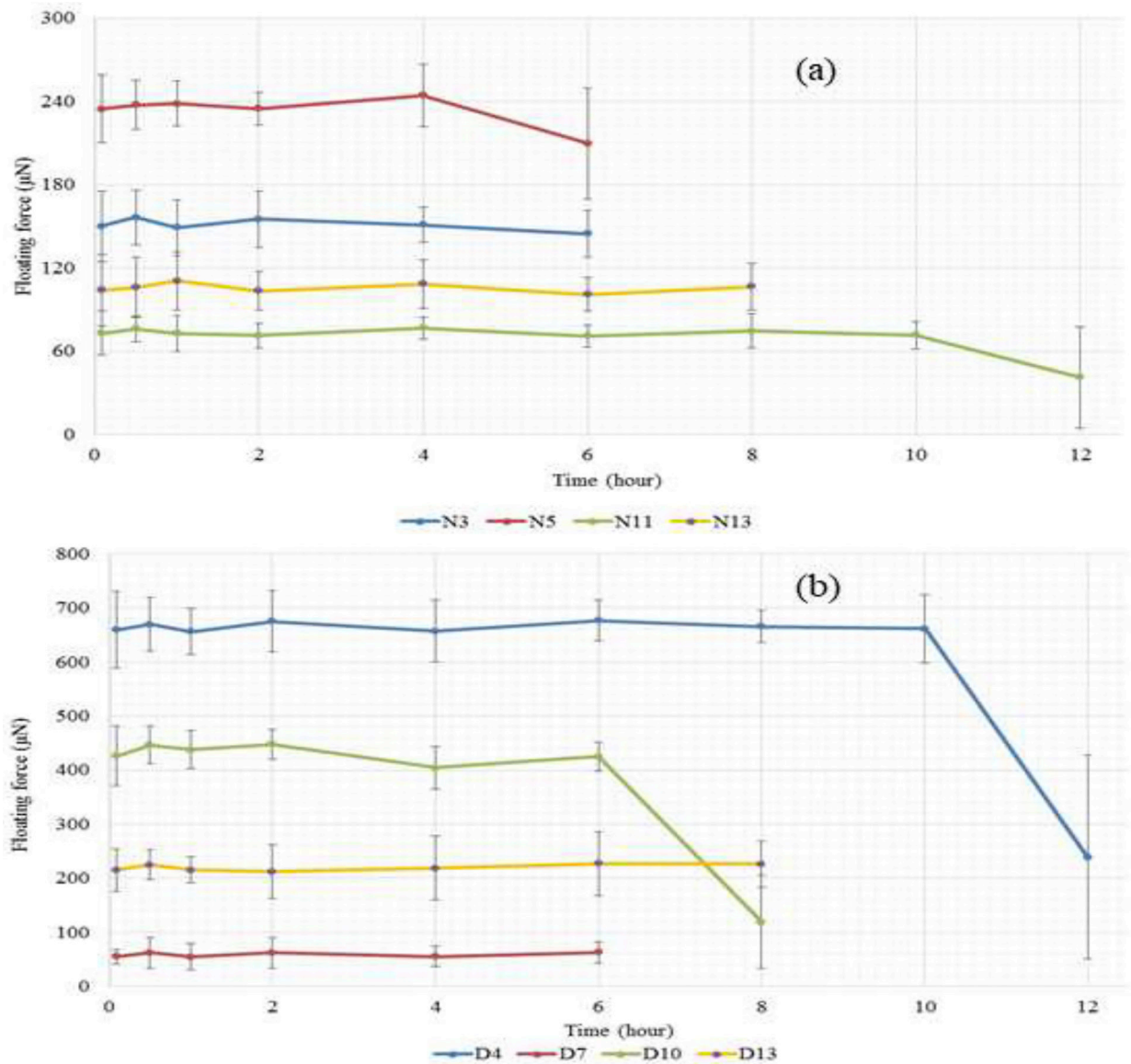


Figure 3:

(a) Representative floating kinetic profiles of printed tablets with the low (N11), medium (N3), high (N5) floating force and that of the center formulation (N13) of the DOE set determining effect of shell, top/bottom, and infill on the floating force of the 3D printed tablets. Data presented as average \pm SD (n=3); (b) Representative floating kinetic profiles of printed tablets with the low (D7), medium (D10), high (D4) floating force and that of the center formulation (D13) of the DOE set determining effect diameter, height, and wall thickness to the floating force of the 3D print tablets

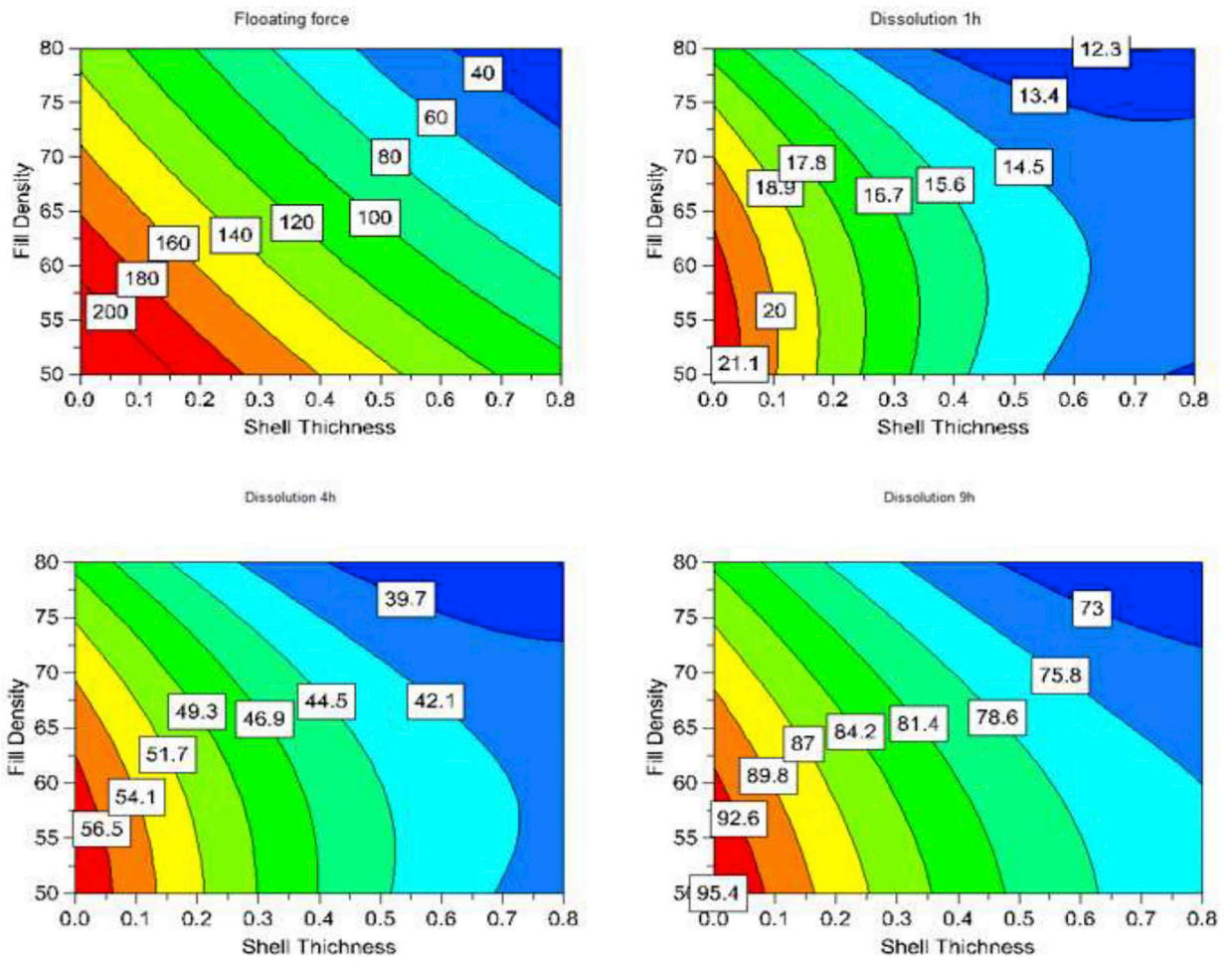


Figure 4: Representative 2D contours describing impacts of printing parameters to performance of printed tablets at different time points.

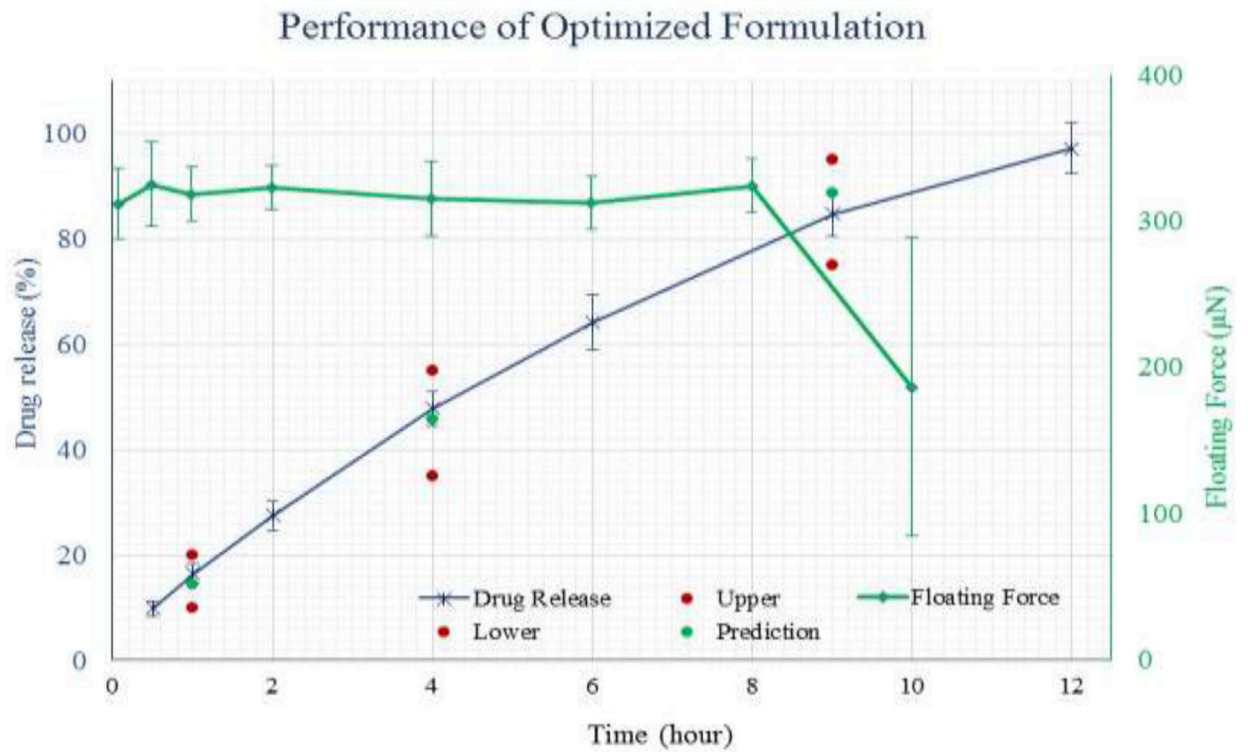


Figure 5: Dissolution profile and floating kinetics of the optimized tablet targeted at weight 400mg; floating force 300 μN ; dissolution 15, 45, 85% at 1, 4, and 9h respectively.

Table 1:

Effect of polymer combination on physical properties of filament.

PVP VA64 Content (%)	Diameter (mm)	Tensile strength (N/mm²)	Uniform strain (%)	Fracture stress (N/mm²)	Strain to fracture (%)	Modulus of rigidity (N/mm²)
0	1.73 ± 0.03	1.94 ± 0.08	50.3 ± 0.8	N/A	N/A	10.8 ± 0.5
20	1.69 ± 0.02	2.79 ± 0.03	56.1 ± 3.3	N/A	N/A	13.5 ± 0.9
40	1.71 ± 0.02	4.30 ± 0.09	54.7 ± 2.9	4.27 ± 0.04	56.1 ± 3.1	21.7 ± 0.7

N/A: The extruded strand was not fracture within the testing strain.

Author Manuscript

Author Manuscript

Author Manuscript

Author Manuscript

Table 2:

Effect of printing parameters on performance of DoE formulations (n=3).

Exp.	Shell Thicknes (mm)	Top/Bottom s Thickness (mm)	Infill Density (%)	Rating force* (μ N)	Dissolution 1h (%)	Dissolution 4h (%)	Dissolution 9h (%)
N1	0.0	0.3	65	183 \pm 31	22.9 \pm 2.2	59 \pm 4.0	94 \pm 5.0
N2	0.8	0.3	65	96 \pm 15	15.2 \pm 1.7	42.2 \pm 2.4	78.8 \pm 4.1
N3	0.0	0.9	65	150 \pm 25	19.7 \pm 2.2	52.8 \pm 1.9	89.5 \pm 3.7
N4	0.8	0.9	65	24 \pm 4	14.3 \pm 1.3	40.3 \pm 4.3	71.8 \pm 3.0
N5	0.0	0.6	50	235 \pm 25	22.3 \pm 1.5	60 \pm 2.2	95.7 \pm 5.5
N6	0.8	0.6	50	99 \pm 22	13.3 \pm 1.1	41.6 \pm 4.0	77.2 \pm 3.7
N7	0.0	0.6	80	136 \pm 29	17.0 \pm 1.0	48.3 \pm 2.4	84.4 \pm 3.5
N8	0.8	0.6	80	18 \pm 4	12.1 \pm 1.0	37.2 \pm 2.5	69.2 \pm 3.0
N9	0.4	0.3	50	217 \pm 36	16.6 \pm 1.8	48.9 \pm 2.1	85.8 \pm 4.9
N10	0.4	0.9	50	100 \pm 23	16.1 \pm 1.7	45.3 \pm 4.1	78.4 \pm 4.3
N11	0.4	0.3	80	73 \pm 16	14.2 \pm 1.3	41.7 \pm 3.7	75.1 \pm 3.5
N12	0.4	0.9	80	49 \pm 8	14.0 \pm 1.3	40.6 \pm 2.8	74.1 \pm 3.9
N13	0.4	0.6	65	104 \pm 26	15.7 \pm 1.7	46.1 \pm 3.6	81.3 \pm 3.3
N14	0.4	0.6	65	113 \pm 24	15.2 \pm 1.1	45.8 \pm 2.4	81.5 \pm 4.1

* Floating force was measured at 5 min after tablets was introduced to FaSSGF

Table 3:

Correlation of printing parameter and printed tablet performance.

Variable	Floating force		Dissolution 1h		Dissolution 4h		Dissolution 9h	
	Coeff.	P	Coeff.	P	Co-ff.	P	Coeff.	P
Constant	111.01	0.000	15.73	0.000	45.32	0.000	80.12	0.000
Shell *	-44.52	0.000	-2.58	0.000	-5.47	0.000	-6.19	0.000
T/B **	-22.92	0.000	-0.43	0.086	-1.31	0.014	-1.92	0.010
Fill ***	-34.61	0.000	-1.02	0.004	-2.62	0.001	-3.44	0.001
She *She	5.31	0.145	0.10	0.006	1.80	0.006	1.70	0.023
T/B *T/B	-4.21	0.230	0.27	0.270	0.34	0.421	0.14	0.805
Fill *Fill	1.64	0.618	-0.70	0.024	-1.13	0.035	-0.89	0.152
She *T/B	-6.60	0.076	0.30	0.211	0.33	0.421	0.04	0.939
She *Fill	1.27	0.686	0.52	0.056	0.91	0.061	0.81	0.171
T/B *Fill	13.43	0.006	0.05	0.824	0.44	0.297	0.85	0.154
	Q2 = 0.710		Q2 = 0.652		Q2 = 0.543		Q2 = 0.492	
	R2 = 0.990		R2 = 0.980		R2 = 0.986		R2 = 0.981	

* shell thickness,

** top/bottom thickness,

*** infill percentage

Table 4:

Effect of model design on weight, floating force, and dissolution of floating tablets (n=3).

Exp.	Diamete (mm)	Height (mm)	Wall Thickenss (mm)	Floating force* (μ N)	Dissolution 1h (%)	Dissolution 4h (%)	Dissolution 9h (%)
D1	8	5.0	1.6	30 \pm 06	18.6 \pm 1.0	61.0 \pm 4.4	97.2 \pm 4.7
D2	12	5.0	1.6	304 \pm 42	14.7 \pm 1.2	46.4 \pm 2.5	83.0 \pm 3.9
D3	8	8.0	1.6	90 \pm 21	16.8 \pm 1.5	54.3 \pm 3.3	90.2 \pm 4.0
D4	12	8.0	1.6	659 \pm 71	15.4 \pm 1.7	45.5 \pm 4.0	81.3 \pm 3.3
D5	8	6.5	1.2	125 \pm 18	17.1 \pm 1.1	59.0 \pm 2.7	96.7 \pm 5.1
D6	12	6.5	1.2	648 \pm 78	14.6 \pm 1.6	46.4 \pm 2.5	84.0 \pm 5.0
D7	8	6.5	2.0	55 \pm 13	16.1 \pm 1.5	55.5 \pm 4.5	91.9 \pm 4.5
D8	12	6.5	2.0	312 \pm 44	13.9 \pm 1.4	41.6 \pm 3.1	78.7 \pm 4.1
D9	10	5.0	1.2	228 \pm 47	18.6 \pm 0.8	58.8 \pm 5.0	94.5 \pm 4.2
D10	10	8.0	1.2	426 \pm 55	17.8 \pm 1.3	54.7 \pm 2.8	89.1 \pm 4.0
D11	10	5.0	2.0	98 \pm 19	16.2 \pm 1.1	52.6 \pm 2.7	89.2 \pm 3.9
D12	10	8.0	2.0	253 \pm 50	15.7 \pm 1.9	50.2 \pm 2.7	87.2 \pm 5.2
D13	10	6.5	1.6	215 \pm 40	16.0 \pm 0.8	52.2 \pm 3.8	89.9 \pm 5.4
D14	10	6.5	1.6	209 \pm 31	16.1 \pm 0.9	52.4 \pm 2.9	89.5 \pm 3.1
D15	10	6.5	1.6	218 \pm 47	16.5 \pm 1.3	52.8 \pm 4.6	89.0 \pm 2.9

* Floating force was measured at 5 min after tablets was introduced to FaSGF

Table 5:

Correlation of printing parameter and printed tablet performance.

Variable	Weight		Floating force		Dissolution 1h		Dissolutio n 4h		Dissolution 9h	
	Coeff.	P	Coeff	P	Coeff.	P	Coeff	P	Coeff.	P
Const.	345.26	0.000	220.60	0.000	16.269	0.000	52.383	0.000	88.944	0.000
D	104.94	0.000	153.38	0.000	-0.952	0.001	-4.651	0.000	-4.619	0.000
H	39.58	0.000	72.79	0.000	-0.231	0.129	-1.451	0.001	-1.511	0.006
W	20.96	0.004	-67.29	0.000	-0.571	0.006	-1.862	0.000	-1.641	0.004
D*D	8.03	0.151	24.03	0.016	-0.445	0.025	-1.199	0.003	-0.989	0.041
H*H	7.60	0.170	3.77	0.598	0.466	0.021	0.880	0.010	0.584	0.167
W*W	-8.12	0.141	12.28	0.126	-0.020	0.895	0.162	0.492	0.211	0.584
D*H	7.89	0.144	42.89	0.001	0.387	0.036	0.717	0.019	0.463	0.239
D*W	9.36	0.095	-37.77	0.002	0.035	0.808	-0.174	0.446	-0.237	0.525
H*W	-0.70	0.885	-5.77	0.410	0.073	0.614	0.180	0.431	0.143	0.698
	Q2 = 0.838		Q2 = 0.854		Q2 = 0.667		Q2 = 0.724		Q2 = 0.574	
	R2 = 0.993		R2 = 0.995		R2 = 0.957		R2 = 0.994		R2 = 0.981	

(D: tablet diameter; H: tablet height; W: wall thickness)